

# Supplemental Material of “Emergent periodic and quasiperiodic lattices on surfaces of synthetic Hall tori and synthetic Hall cylinders”

Yangqian Yan,<sup>1</sup> Shao-Liang Zhang,<sup>2</sup> Sayan Choudhury,<sup>1</sup> and Qi Zhou<sup>1</sup>

<sup>1</sup>*Department of Physics and Astronomy, Purdue University, West Lafayette, IN, 47907*

<sup>2</sup>*School of Physics, Huazhong University of Science and Technology, Wuhan 430074, People’s Republic of China*

The notation employed in this Supplemental Material follows that introduced in the main text. Section I used the non-abelian Wilson line technique to clarify why the crossing is avoided in Fig. 2 of the main text. Section II clarifies the parameters used in the simulation in Fig. 4 of the main text. Section III provides an alternative simulation: expansion of the ground state in a 1D harmonic trap. Section IV provides a full 3D simulation of a proposed experiment to demonstrate the localization of the ground state due to gluing of two cylinders. Section V clarifies Fig. 2(a-b) in the main text.

## I. BLOCH OSCILLATIONS IN THE PRESENCE OF BAND CROSSINGS

In the presence of a constant force,  $F$ , the quasi-momentum becomes  $k_f = k_0 + Ft$  at time  $t$ , where  $k_0$  is the initial quasi-momentum at  $t = 0$ . In the adiabatic limit, the inter-band transition can be determined by the path-ordered integral [1, 2],

$$W(k_f; k_0) = \hat{P} \exp[i \int_{k_0}^{k_f} \hat{A}(k) dk / \hbar], \quad (\text{S1})$$

where  $\hat{P}$  is the path-ordering operator and the matrix representation of the non-Abelian Berry connection  $\hat{A}(k)$  is defined as  $A_{s',s}(k) = \langle \bar{u}_{s'k} | i \partial_k | \bar{u}_{sk} \rangle$ , where  $|\bar{u}_{sk}\rangle$  is the periodic Bloch wavefunction in the  $s$ th band,

$$|\bar{u}_{sk}\rangle = e^{isq_L x} \sum_{j=1}^M \sum_l \tilde{c}_{l,s}^j(k) e^{ilQx} |j\rangle. \quad (\text{S2})$$

We obtain

$$A_{s',s}(k) = \sum_j \sum_{l,l'}^M \left( \tilde{c}_{l',s'}^{j*}(k) \partial_k \tilde{c}_{l,s}^j(k) \right) \int_0^{2\pi/q_L} e^{i[(s-s')q_L + (l-l')Q]x} dx \sim \delta((s-s')q_L + (l-l')Q). \quad (\text{S3})$$

As  $|s-s'|q_L \leq (n-1)q_L$  and  $|l-l'|Q \geq nq_L$  (if  $l \neq l'$ ), to ensure that  $(s-s')q_L + (l-l')Q = 0$  is valid,  $s = s'$  and  $l = l'$  must be satisfied. Thus,  $A_{s',s}(k) \sim \delta(s-s')$ ; Here,  $n = Q/q_L$  is defined in the main text. This means that during the time evolution, there is no transition between bands with different  $s$  (different colored bands in Fig. 2 of the main text).

## II. INTERACTION EFFECTS ON THE EXPANSION OF A GAUSSIAN WAVE PACKET IN THE REAL SPACE

As discussed in the main text, we consider a Gaussian wave packet as the initial state. All the spin components have equal amplitude and phase. The width of the wave packet,  $\sigma_0 = \sqrt{\langle x^2 \rangle - \langle x \rangle^2}$ , is  $455/q$ . We use  $\gamma_8 = 13/21$  to approximate  $\gamma$ . The density spread  $\sigma_0$  is roughly 3.5 times the underlying period of the Hamilto-

nian. Figure S1 shows the ratio of the width in a later time  $t$  to  $\sigma_0$ , where  $t = 1000\hbar/E_r$ , as a function of the initial interaction energy  $E_i = \int g\rho_i^2 dx$  for  $\Omega' = 0$  and  $\Omega' = 2E_r$ . In both cases, weak attractive (repulsive) interactions decrease (increase) the width,  $\sigma(t)$ . When in-

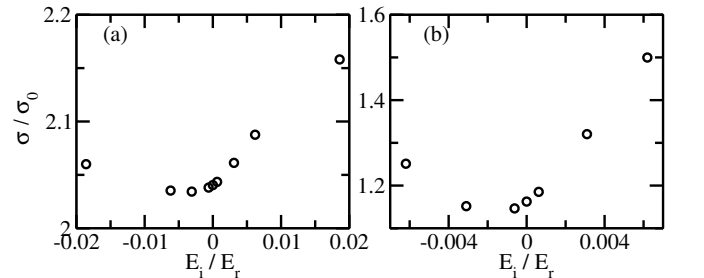


FIG. S1. Density spread as a function of initial interaction energy  $E_i$  for  $\Omega' = 0$  (a) and  $\Omega' = 2E_r$  (b).

interactions are strong enough, the width always increase with increasing the strengths of interactions due to the mixing with extended states at high energies.

### III. EXPANSION DYNAMICS OF THE GROUND STATE IN A HARMONIC TRAP

We consider weakly interacting bosons in a harmonic trap with the trapping frequency  $\omega = 0.034E_r/\hbar$ , and use the imaginary time propagation to find the ground state. For non-interacting systems, the ground state has a Gaussian profile. In the presence of a weak repulsive interaction, the density is featured with a Thomas-Fermi profile.

Then we turn off the trap and the interactions, and let the cloud expand. Fig. S2 shows the width of the wavepacket as a function of time. When  $\Omega' = 0$ , the ground state in the trap is an extended one. Therefore, the wavepacket expands quickly after the trap and interactions are turned off. In contrast, when  $\Omega' = 2E_r$ , the ground state is a localized one. Even after turning off the trap and interaction, the width of the wavepacket has little changes, well reflecting the localized nature of the ground state in the trap. As a further comparison, we turn on a weak interaction in the expansion dynamics once the trap is turned off. It is clear that a weak repulsive interaction speeds up the expansion and a weak attractive interaction slows it down.

All these results are similar to those presented in the main text. It means that a shallow trap used in typical cold atom experiments do not change our qualitative results and main conclusions. In a shallow trap, though the momentum is no longer a good quantum number and an extended state does not extend to infinity, it can still spread over the whole trap. In contrast, localized states still remain localized, provided that the trapping potential is much smaller than the energy gap between the localized states and delocalized ones.

### IV. A REALISTIC SETUP IN EXPERIMENTS

Our scheme can be realized in laboratories as a simple generalization of some current experiments [3]. We choose four hyperfine states of  $^{87}\text{Rb}$ ,  $|F, m_F\rangle = |2, 2\rangle, |2, 1\rangle, |1, 0\rangle, |1, 1\rangle$ . States  $|2, 2\rangle$  and  $|2, 1\rangle$  are resonantly coupled by one pair of counter propagating Raman beams with recoil momentum  $k_r = 2\pi/\lambda$ , where  $\lambda = 790\text{nm}$  is the wavelength. The momentum transferred is  $2k_r$ . States  $|1, 0\rangle$  and  $|1, 1\rangle$  are resonantly coupled by another pair of Raman beams with the same wavelength that is tilted with a small angle  $\theta$  with respect to the first pair of Raman beams. The momentum transferred is  $2k_r \cos\theta$ , where the angle  $\theta$  is chosen such that  $\cos\theta$  is irrational or rational, say,  $\cos\theta = \gamma_i$ , where  $\gamma_i$  is defined in the main text. One microwave couples states  $|2, 2\rangle$  and  $|1, 1\rangle$ , and another couples states  $|2, 1\rangle$

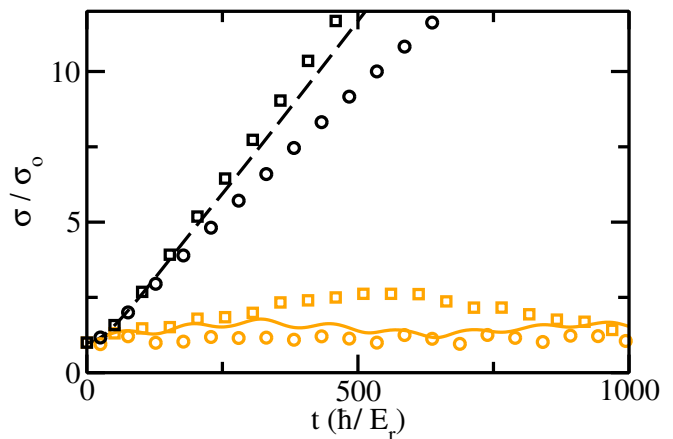


FIG. S2. The evolution of the wavepacket after releasing from the trap. The solid orange (black dashed) curve represents results for  $\Omega' = 2E_r$  ( $\Omega' = 0$ ) when the interaction is also turned off in the expansion. Squares and circles represent results for a small repulsion and a small attractive interaction added in the expansion, respectively. The absolute interaction strength,  $|g|$ , is the same, and the interaction energies  $E_i = \int g\rho_i^2 dx$  differ because of different densities. For  $\Omega' = 2E_r$ ,  $E_i/E_r \approx 0.010$  and  $-0.039$  for positive and negative  $g$ , respectively. For  $\Omega' = 0$ ,  $E_i/E_r \approx 0.0098$  and  $-0.013$  for positive and negative  $g$ , respectively.

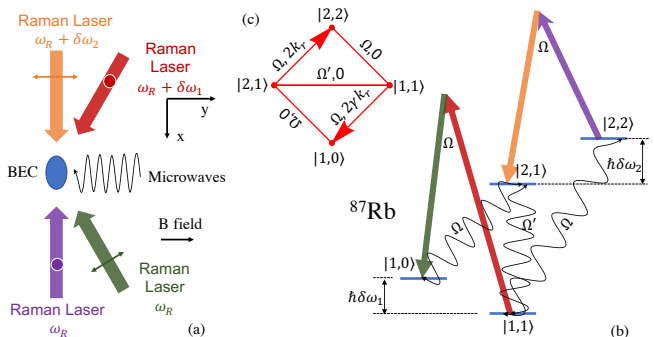


FIG. S3. (a) A Bose Einstein Condensate is confined in a harmonic trap. Straight arrows represent Raman lasers and wiggles indicate microwaves. (b) A scheme to couple hyperfine states of  $^{87}\text{Rb}$ . Four states are cyclically coupled by pairs of Raman lasers (arrows) and microwaves (wiggles). In addition, a microwave couples states  $|1, 1\rangle$  and  $|2, 1\rangle$  with coupling strength  $\Omega'$ . (c) A schematic of the cross sections of two cylinders or tori when they are glued together. The coupling strengths and momenta transferred are labeled.

and  $|1, 0\rangle$ . This completes a cyclic coupling between four states and delivers a synthetic cylinder. Replacing Raman beams by LG beams, this creates a synthetic torus. All coupling strengths are scaled with  $2E_r = \hbar^2(2k_r)^2/m$ , where  $m$  is the mass of a Rubidium atom. As discussed in the main text, eigenstates are extended, even when  $\cos\theta$  is irrational and the Hamiltonian is quasi-periodic.

To glue two cylinders or tori, an extra microwave coupling between states  $|2, 1\rangle$  and  $|1, 1\rangle$  could be added. The

coupling strength is  $\Omega'$ . The experimental setup is depicted in Fig. S3.

Using realistic experimental parameters, we perform time-dependent simulations using the Gross-Pitaevskii equation. We consider 15000  $^{87}\text{Rb}$  atoms in a three-dimensional harmonic trap with an angular trapping frequency  $2\pi \times 500\text{Hz}$ . We compute the ground states in the presence of Raman and microwave couplings, interactions and the harmonic trap. After the initial state is prepared, we turn off the trap along  $\hat{x}$ , the direction of momentum transfer. The transverse confinement remains. All the inter- and intra-species scattering lengths are well approximated by  $93a_0$ , where  $a_0$  is the Bohr radius. The angle is chosen such that  $\cos\theta = 13/21$ .

Fig. S4 shows the width of the wavepacket,  $\sigma$ , as a function of time  $t$  after the trap and the interaction are turned off. The wavepacket expands fast when  $\Omega' = 0$ , as a consequence of the extended ground state in the trap. It expands little when  $\Omega' = 2E_r$ , reflecting the localized nature of the initial state in the trap after glueing two cylinders.

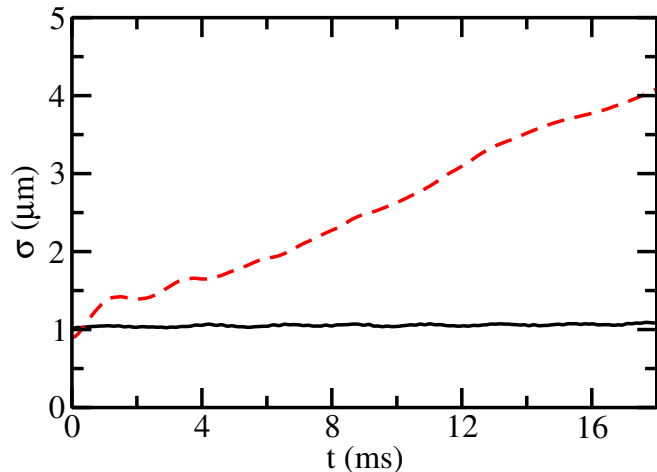


FIG. S4. Expansion dynamics when the ground state is released from the trap along the  $x$  direction. Solid line and dashed lines represent results of  $\Omega' = 2E_r$  and  $\Omega' = 0$ , respectively.

## V. COMPARISONS BETWEEN THE UNIFORM AND NONUNIFORM FLUX

The ground states of the systems for Fig. 2(a) and Fig. 2(b) in the main text are depicted in Fig. S5(a).

The density modulation of each spin component is determined by the total momentum  $Q$ , or equivalently, the total flux penetrating a unit length. The period of the density oscillation  $\tilde{d} = 2\pi/Q$ . However, the relative phases between different spin components depend on how the flux is distributed on the surface. For the system in Fig. 2(a),  $n = 3$ ,  $q_L = q = Q/3$ , and the flux is uniformly distributed. The relative phase has a pe-

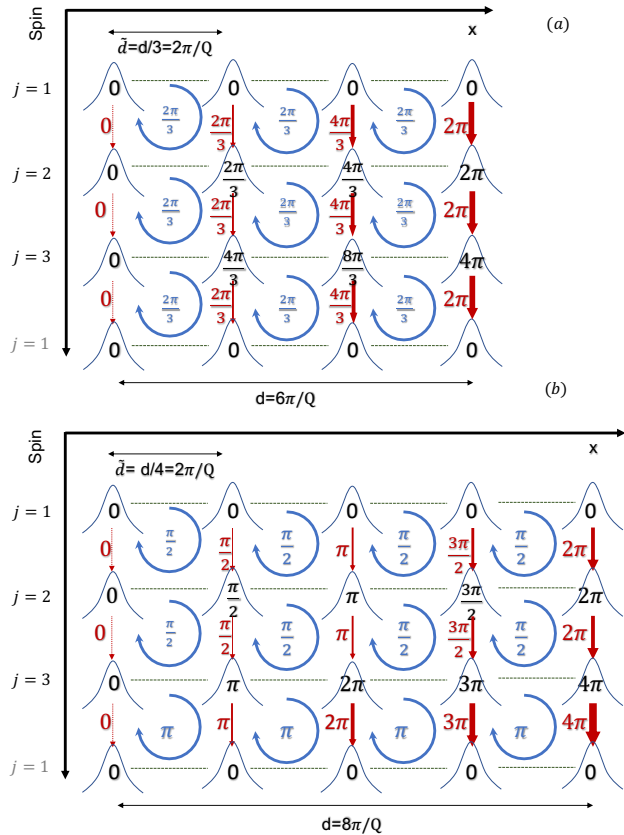


FIG. S5. Curves represent the density profiles of each individual spin component near the maxima. The phases of the wavefunctions are also shown. Red arrows represent the spatially dependent coupling along the synthetic direction. Maxima of the density form plaquettes, in which the flux per plaquette are shown.

riod of  $d = 2\pi/q = 3\tilde{d}$ . The lattice spacing is therefore  $d = 6\pi/Q$ . In contrast, for the system in Fig. 2(b),  $n = 4$ ,  $q_L = 3q/4$ , and the distribution of the flux is nonuniform. The relative phase has a period of  $8\pi/Q$ , and the lattice spacing is therefore  $8\pi/Q$ .

[1] T. Li, L. Duca, M. Reitter, F. Grusdt, E. Demler, M. Endres, M. Schleier-Smith, I. Bloch, and U. Schneider, Bloch state tomography using Wilson lines. *Science* **352**, 1094 (2016).

[2] S.-L. Zhang and Q. Zhou, Two-leg Su-Schrieffer-Heeger chain with glide reflection symmetry, *Phys. Rev. A* **95**, 061601(R) (2017).

- [3] C.-H. Li, Y. Yan, S. Choudhury, D. B. Blasing, Q. Zhou, and Y. P. Chen, A Bose-Einstein Condensate on a Synthetic Hall Cylinder, [arXiv:1809.02122](https://arxiv.org/abs/1809.02122).